BJO Online First, published on April 2, 2015 as 10.1136/bjophthalmol-2014-306237

Morpho-functional correlation of fundus autofluorescence in Stargardt disease

Maurizio Battaglia Parodi,[1] Pierluigi Iacono,[2] Giacinto Triolo,[1] Carlo La Spina,[1] Ilaria Zucchiatti,[1] Maria Vittoria Cicinelli,[1] Enrico Borrelli,[1] Maria Pia Manitto,[1] Elisabetta Martina,[1] Francesco Bandello[1]

[1]Department of Ophthalmology, University Vita-Salute, Scientific Institute San Raffaele, Milano, Italy
[2]Department of Ophthalmology, Fondazione G. B. Bietti per l'Oftalmologia, IRCCS (Istituto di Ricovero e Cura a Carattere Scientifico), Rome, Italy

Correspondence to
Dr Pierluigi Iacono, Department of Ophthalmology, Fondazione G. B. Bietti per l'Oftalmologia, IRCCS (Istituto di Ricovero e Cura a Carattere Scientifico), Via Livenza 3, Rome 00198, Italy; pierluigi.iacono@libero.it

Received 7 October 2014
Revised 12 March 2015
Accepted 21 March 2015

ABSTRACT

Background To correlate patterns in short-wavelength (SW) and near-infrared (NIR) fundus autofluorescence (FAF) with morpho-functional outcomes in eyes affected by Stargardt disease.

Methods Fifty-four eyes of 27 patients were prospectively enrolled. All patients underwent a complete ophthalmologic examination including SW-FAF, NIR-FAF, microperimetry and spectral-domain optical coherence tomography (SD-OCT). The main outcome measures were identification of a correlation between NIR-FAF and SW-FAF patterns within the foveal region and best corrected visual acuity (BCVA) values. Secondary outcome measures were correlation of FAF patterns with SD-OCT findings and retinal sensitivity on microperimetry.

Results Eyes showing a pattern of foveal hyper-FAF on NIR-FAF had a higher BCVA than eyes with a reduced FAF signal (0.44±0.23 LogMAR vs 1.08±0.19, p<0.001). Similarly, mean sensitivity within 2° of the foveal region was significantly better (6.45±2.39 dB) in eyes with hyper-FAF than in eyes with hypo-FAF (0.23 ±0.45 dB, p<0.001). Moreover, eyes with hyper-FAF on SW-FAF did not present a significant difference in BCVA (0.73±0.31 vs 0.83±0.43, p=0.335) and mean retinal sensitivity (4.34±3.91 dB vs 2.33±2.96, p=0.07) compared with the subgroup with foveal hypo-FAF. The integrity of both the photoreceptor inner/outer segment junction and the photoreceptor outer segment/retinal pigmented epithelium junction was significantly correlated with a preserved BCVA and a foveal hyper-FAF pattern on NIR-FAF.

Conclusions Our data suggest that NIR-FAF patterns correlate with morpho-functional outcomes in eyes affected by Stargardt disease. Longitudinal investigations are warranted to assess more precisely the actual contribution of NIR-FAF in the clinical characterisation of Stargardt disease.

INTRODUCTION

Stargardt disease (STGD) is a retinal dystrophy characterised by progressive loss of central visual function. STGD is most commonly inherited as an autosomal recessive trait, and generally has an onset in childhood or young adulthood.[1–3]

STGD is caused by mutations in the gene encoding the photoreceptor cell-specific ATP-binding cassette transporter (ABCA4),[4 5] a protein that enables vitamin A derivatives to be transported through the outer segment disc membranes. A defective RIM protein encoded by the ABCA4 gene results in abnormal degradation of visual cycle by-products, leading to lipofuscin accumulation within the retinal pigment epithelium (RPE).[6] Final RPE and photoreceptor degeneration are brought about by toxic effects due to lipofuscin storage.[7 8]

The most common phenotypic presentation of STGD includes foveal atrophy, surrounded by flecks clearly visible as paramacular yellow deposits. The retinal function and the anatomical appearance of STGD varies widely among patients, according to the severity of the disease. Several diagnostic tools have been proposed as a means of assessing the macular dysfunction.

Fundus autofluorescence (FAF) enables the visualisation of A2E and other bisretinoid components of lipofuscin in the RPE.[9 10] In particular, short-wavelength FAF (SW-FAF) in STGD is typically characterised by a general increase at the onset of the disease, with specific hyper-autofluorescence (hyper-AF) at the flecks level, and decreased FAF, as long as the central atrophic change takes place.[11–19] In addition to SW-FAF, near-infrared FAF (NIR-FAF)[20 21] has also been applied to STGD to visualise the alterations of melanin within the RPE cells.[15 22 23]

Although many studies have described the distinctive abnormalities of FAF in STGD, the information available that can help to draw a parallel between FAF patterns and functional outcomes is limited.

The purpose of this study is to correlate SW-FAF and NIR-FAF patterns of the foveal region with the functional outcomes in eyes affected by STGD. Our results indicate that a more precise relationship with the visual functions can be provided by the NIR-FAF pattern.

METHODS

A consecutive series of patients affected by STGD were prospectively recruited for the study. Written informed consent was obtained from all subjects. The protocol was approved by the local institutional review board, and the procedures adhered to the tenets of the Declaration of Helsinki.

All patients underwent a complete ophthalmic examination, including best corrected visual acuity (BCVA) on ETDRS charts, applanation tonometry, biomicroscopic examination, SW-FAF, NIR-\FAF, spectral-domain OCT (SD-OCT) and microperimetry. Patients were excluded from the study if they had significant cataracts or other media opacities, and/or if they had other ocular diseases that could affect the results.

To cite: Parodi MB, Iacono P, Triolo G, *et al*. *Br J Ophthalmol* Published Online First: [*please include* Day Month Year] doi:10.1136/bjophthalmol-2014-306237

Table 1 Demographic data and molecular genetic status of 27 patients with Stargardt disease

Patient	Age	Onset	Variant identified
1	18	12	c.5461-10 T>C
2	20	10	p.Phe418Ser
3	45	20	Arg212Cys/p.Gly1961Glu
4	34	17	p.Leu541Pro
5	14	12	p.Asn96Asp/p.Gly2074Ser
6	45	13	p.Asn96Asp/p.Gly2074Ser
7	45	12	p.Arg1640Trp/p.Leu2027Phe
8	40	15	c.5461-10 T>C
9	43	20	pAla1598Asp
10	23	16	p.Cys54Tyr
11	27	16	p.Gly863Ala
12	28	14	p.Asn965Se
13	38	16	p.Cys2150Tyr
14	41	23	p.His423Arg
15	23	12	pAla1598Asp
16	23	11	p.Leu541Pro
17	34	10	p.His423Arg
18	46	26	p.Gly2074Ser
19	35	23	p.Leu541Pro/ p.Ala1038Va/ p.Gly1961Glu
20	51	21	Arg212Cys
21	51	19	p.Gly1961Glu
22	45	17	c.5461-10 T>C
23	43	18	p.Ala1038Va
24	18	9	p.Pro1380Leu
25	16	9	Arg212Cys
26	21	9	p.His423Arg
27	20	10	p.Pro1380Leu

The diagnosis of STGD was based on a recorded family history compatible with autosomal recessive inheritance, presence of bilateral impairment of central vision, atrophic macular lesions (beaten bronze appearance or large patches of atrophy) with or without perimacular and/or peripheral white-yellow flecks. STGD was described in accordance with the classification of Fishman *et al*,[24] as follows: phenotype I (small atrophic-appearing foveal lesions and localised perifoveal yellowish-white flecks; phenotype II (numerous yellowish-white fundus lesions throughout the posterior pole); and phenotype III (extensive atrophic-appearing RPE changes). All patients also underwent molecular analyses for gene ABCA4.

FAF was obtained using a confocal scanning laser ophthalmoscope (Heidelberg Retinal Angiograph 2; Heidelberg Engineering, Heidelberg, Germany). NIR-FAF imaging was carried out using a diode laser at 787 nm wavelength for excitation and a barrier filter for detection of emitted light above 810 nm. SW-FAF images of ocular fundi were obtained at 488 nm excitation wavelength, and a barrier filter with wavelength of 500 nm was used for the detection of emitted light.

For SW-FAF and NIR-FAF, 100 single images (30°×30° view mode, 768×768 pixels) were acquired after pupil dilation with 1% tropicamide and averaged to obtain a high-quality image. FAF foveal patterns were classified either as hyper-AF (increased signal with respect to FAF background) or hypo-AF (reduced signal with respect to the FAF background), on both techniques. The analysis and comparison of the FAF images were performed after a complete alignment of SW-FAF and NIR-FAF images, achieved by overlapping the images using commercially available Photoshop software.

SD-OCT was carried out using the Spectralis HRA (Heidelberg Engineering, Heidelberg, Germany), by means of a five-line raster scan and a horizontal line scan centred on the fovea, after pupil dilation with 1% tropicamide. Horizontal scans of 8.7 mm were obtained using the automated retinal tracking system, with 50–100 frames.

The following structures were analysed in particular: photoreceptor inner/outer segment (IS/OS) junction and photoreceptor outer segment/retinal pigmented epithelium (OS/RPE) junction. Each OCT finding within the foveal area was classified as preserved (identification of IS/OS junction), disrupted (IS/OS junction disorganisation) or absent (IS/OS junction loss).

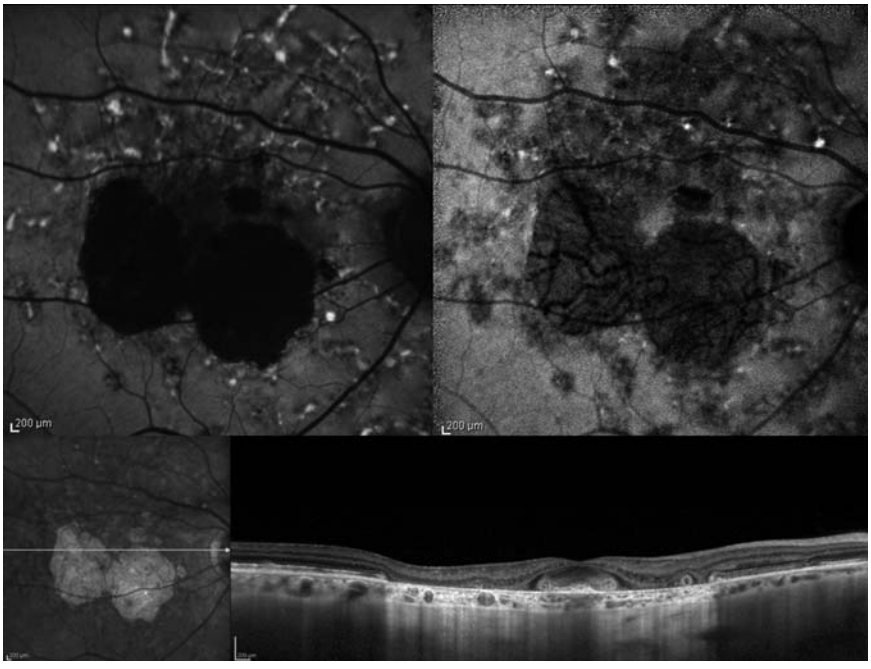

Figure 1 Top left: short-wavelength fundus autofluorescence, showing a wide central hypo-autofluorescence surrounded by several hyper-autofluorescent flecks. Top right: near-infrared fundus autofluorescence of the same eye reveals a hyper-autofluorescent signal corresponding to the foveal area. Bottom: spectral-domain optical coherence tomography discloses the partial preservation of the photoreceptors in the foveal region.

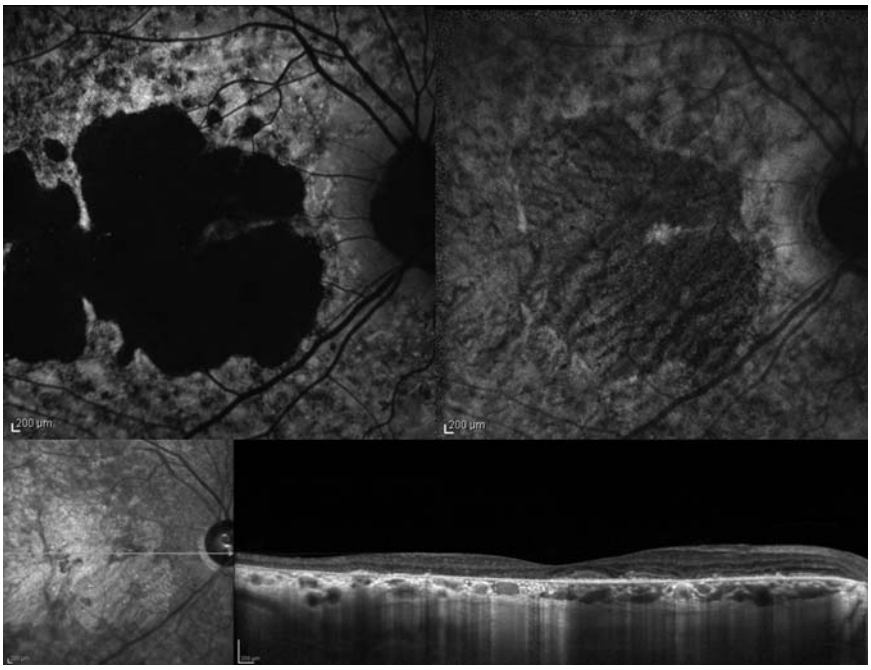

Figure 2 Top left: short-wavelength fundus autofluorescence, revealing a large hypo-autofluorescence centred by a slightly hyper-autofluorescent signal. Top right: near-infrared fundus autofluorescence of the same eye confirms the presence of a hyper-autofluorescent area corresponding to the foveal region. Bottom: spectral-domain optical coherence tomography shows that the photoreceptors in the foveal region are extremely poorly preserved.

Two examiners masked to the purpose of the investigation judged SD-OCT, SW-FAF and NIR-FAF images independently. Cases of diverging interpretation were discussed with a third senior examiner (FB).

Microperimetry was performed using a MP-1 Microperimeter (Nidek Technologies, Padua, Italy) by a single experienced ophthalmologist (GT) in the same dimly lit room conditions. The pupil was dilated and the patients were dark adapted for at least 15 min; each subject enrolled in the study also underwent a pretest training examination. Threshold fundus perimetry was performed employing a 68-stimuli grid covering the central 10° of the retina (figure 2), projecting Goldmann III stimuli size with a 4-2 full threshold projection strategy, with a presentation time of 200 ms and a 1000 ms interval between stimuli. The fixation target consisted of a 2° diameter red cross, and the average retinal sensitivity registered within the 2° of the foveal anatomical region was taken into account for the purpose of the study. During MP-1 testing, automated real-time fundus tracking via infrared fundus imaging served to compensate for misalignment by delaying stimulus projection until realignment was achieved. Fixation stability was calculated as the percentage of fixation points inside the 2°-diameter circle. Eyes with more than 50% of the preferred fixation points detected inside the 2°-diameter circle were categorised as having central fixation; eyes under 50% were classified as having eccentric fixation. In addition, eyes with more than 75% of preferred fixation points inside the 2°-diameter circle were categorised as having stable fixation, whereas eyes with less than 75% were defined as having unstable fixation.

In order to ensure a precise correspondence between retinal sensitivity and FAF patterns, the images were superimposed on the corresponding microperimetry by means of commercially available Photoshop software.

The foveal anatomical region was identified as the area of the foveal retinal depression indicated on the SD-OCT scan. The retinal sensitivity values within the 2° of the foveal anatomical region were considered for the analyses of the FAF patterns.

The primary outcome of the study was the identification of a correlation between NIR-FAF and SW-FAF patterns within the foveal region and BCVA value. The secondary outcome included the appraisal of the correlation of FAF patterns with OCT findings and retinal sensitivity.

The Kruskal–Wallis non-parametric test and Pearson's χ^2 test were used for continuous and categorical variable distribution analysis, respectively. A two-tailed p value <0.05 was taken as statistically significant. All calculations were performed with a GraphPad Prism V.5.00 (GraphPad Software, San Diego, California, USA).

Table 2 Distribution of the fixation according to SW-FAF and NIR-FAF categorisation

Fixation	SW-FAF hypo-AF	SW-FAF hyper-AF	p Value
Eccentric and unstable	15	14	0.80
Central and stable	13	12	
	NIR-FAF hypo-AF	**NIR-FAF hyper-AF**	**p Value**
Eccentric and unstable	27	2	0.0001
Central and stable	2	23	

A correlation was found between FAF patterns and the frequency distribution of the fixations only according to the NIR-FAF categorisation (p=0.0001).
AF, autofluorescence; NIR-FAF, near-infrared fundus autofluorescence; SW-FAF, short wavelength fundus autofluorescence.

RESULTS

Overall, 27 patients (54 eyes) were enrolled. The mean age of the patients was 32±12 years (range 12–51 years) and the mean duration of the disease was 17±7 years (range 4–28 years). Molecular analyses disclosed that all patients had known mutations in the ABCA4 gene (table 1).

Mean BCVA was 0.78±0.38 LogMAR (range 1.30–0.1). Twelve and 15 patients showed phenotypes I and II, respectively. Foveal sparing was registered in eight eyes.

The SW-FAF analysis showed a foveal hypo-AF pattern in 28 cases (52%) and a foveal hyper-AF pattern in 26 eyes (48%) (figures 1 and 2). According to the SW-FAF patterns, a mean BCVA of 0.83±0.43 LogMAR (approximately corresponding to 20/125 Snellen equivalent) was found in eyes with foveal

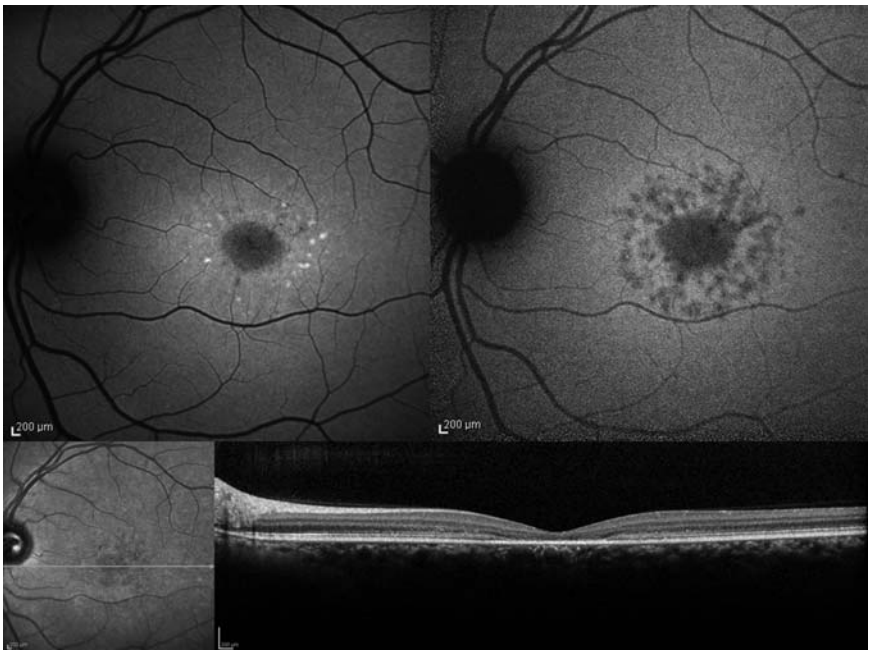

Figure 3 Top left: short-wavelength fundus autofluorescence, revealing a central hypo-autofluorescent area surrounded by many hyper-autofluorescent lesions corresponding to flecks. Top right: near-infrared fundus autofluorescence of the same eye shows a similar response characterised by a central hypo-autofluorescence, even though the flecks appear as hypo-autofluorescent. Bottom: spectral-domain optical coherence tomography reveals the absence of the outer retinal layers in the foveal region.

hypo-AF, whereas an averaged value of 0.73±0.31 LogMAR (approximately corresponding to 20/100 Snellen equivalent) was found in eyes showing a foveal hyper-AF; the difference in the mean BCVA proved not to be statistically significant (p=0.335).

Mean sensitivity of the foveal anatomical region was 2.33 ±2.96 dB in the subgroup with foveal hypo-AF, and 4.34 ±3.91 dB in the subgroup with foveal hyper-AF, with no statistically significant difference (p=0.07). Fixation was central and stable in 13 and 12 eyes showing, respectively, hypo-AF and hyper-AF, whereas it was eccentric and unstable in 15 and 14 eyes showing hypo-AF and hyper-AF, respectively, with no statistically significant difference in frequency distribution in each pattern (table 2, χ^2 test, p=0.80).

NIR-FAF disclosed a hypo-AF pattern within the foveal area in 29 cases (53%) and a foveal hyper-AF pattern in 25 eyes (47%) (figures 2 and 3).

According to the NIR-FAF classification, the mean BCVA was 0.44±0.23 LogMAR (approximately corresponding to 20/50 Snellen equivalent) in the eyes showing a foveal hyper-AF, whereas it was 1.08±0.19 LogMAR (approximately corresponding to 20/250 Snellen equivalent) in eyes displaying a foveal hypo-AF (p<0.001). Mean sensitivity within the foveal anatomical region was 6.45±2.39 dB in the subgroup with foveal hyper-AF, and 0.23±0.45 dB in the subgroup with foveal hypo-AF (p<0.001). Fixation was central and stable in just 2 eyes with NIR-hypo-AF and in 23 eyes with NIR-hyper-AF; fixation was found to be eccentric and unstable in 27 eyes with hypo-AF and in 2 hyper-AF eyes, with a statistically significant difference in frequency distribution in each pattern (table 2, χ^2 test, p=0.0001).

Moreover, a BCVA≤1 LogMAR (approximately corresponding to 20/200 Snellen equivalent) was found in 27 out of 29 eyes (93%) showing a foveal hypo-AF on NIR-FAF, whereas it was registered in 14 out of 28 (50%) eyes with foveal hypo-AF on SW-FAF, with a statistically significant difference (p<0.001).

Comparison of the BCVA and of the integrity of the IS/OS and OS/RPE layers identified a correlation between the disarrangement of IS/OS and OS/RPE layers and a decreased BCVA. In detail, eyes characterised by an absent or disrupted IS/OS layer displayed a BCVA of 0.92±0.12 LogMAR (approximately corresponding to 20/160 Snellen equivalent), whereas those with a normal IS/OS layer showed a BCVA of 0.52±0.25 LogMAR (approximately corresponding to 20/65 Snellen equivalent) (p<0.001). Similarly, eyes with OS/RPE layer disruption or absence revealed a BCVA of 0.90±0.13 LogMAR (approximately corresponding to 20/160 Snellen equivalent), whereas those with a normal OS/RPE finding showed a BCVA of 0.58±0.17 LogMAR (approximately corresponding to 20/80 Snellen equivalent) (p<0.001).

As listed in table 3, preserved IS/OS and OS/RPE layers were more frequently associated with a foveal NIR-hyper-AF (p=0.001); however, taking into account the two main patterns on SW-FAF, no statistically significant relationship was found between the examined SD-OCT findings and SW-FAF analysis (p=0.216).

Table 3 Frequency distribution of the alterations of the IS/OS and OS/RPE layers according to the FAF patterns

OCT findings	SW-FAF hypo-AF	SW-FAF Hyper-AF
IS/OS absent	15 (53%)	8 (31%)
IS/OS disrupted	10 (36%)	16 (61%)
IS/OS preserved	3 (11%)	2 (8%)
	NIR-FAF hypo-AF	**NIR-FAF hyper-AF**
IS/OS absent	24 (83%)	1 (4%)
IS/OS disrupted	4 (14%)	20 (80%)
IS/OS preserved	1 (3%)	4 (16%)
	SW-FAF hypo-AF	**SW-FAF hyper-AF**
OS/RPE absent	16 (57%)	4 (15%)
OS/RPE disrupted	7 (25%)	20 (77%)
OS/RPE preserved	5 (18%)	2 (8%)
	NIR-FAF Hypo-AF	**NIR-FAF Hyper-AF**
OS/RPE absent	18 (62%)	2 (8%)
OS/RPE disrupted	10 (35%)	17 (68%)
OS/RPE preserved	1 (3%)	6 (24%)

A correlation was found between NIR-FAF patterns and OCT findings (p<0.001). No correlation was registered between SW-FAF patterns and OCT findings (p=0.216).
AF, autofluorescence; IS/OS, inner segment/outer Segment; NIR-FAF, near-infrared fundus autofluorescence; OCT, optical coherence tomography; OS/RPE, outer segment/retinal pigment epithelium; SW-FAF, short wavelength fundus autofluorescence.

DISCUSSION

FAF is considered the most useful non-invasive imaging tool for the evaluation of patients affected by STGD.[12–19] In particular, SW-FAF identifies and monitors flecks and areas of RPE atrophy. Moreover, SW-FAF abnormalities show a good correlation with disorganisation or loss of IS/OS junction, as visualised on OCT.[13 19] However, no precise correlation has been established between FAF patterns and functional outcomes.

The purpose of our study was to investigate whether a relationship exists linking foveal FAF patterns with functional and OCT outcomes. The results indicate that BCVA is correlated with the foveal FAF signal, but the most precise correlation can be found between the foveal NIR-FAF pattern and BCVA. In particular, eyes displaying foveal hyper-AF on NIR-FAF have a higher BCVA, whereas, on the contrary, BCVA is ≤1 LogMAR when foveal hypo-AF is detectible on NIR-FAF. A correlation between foveal NIR-FAF and microperimetric data can also be found, since foveal sensitivity is higher in patients showing foveal hyper-AF on NIR-FAF. Analyses of SD-OCT data corroborate these findings. Eyes disclosing foveal hyper-AF on NIR-FAF are less frequently characterised by absence of IS/OS and OS/RPE layers.

The NIR-FAF signal is considered to be principally generated by melanin granule accumulation within the RPE cells.[20 21] The normal NIR-FAF pattern is characterised by a round high fluorescence centred on the fovea.[20 21] Previous investigations have remarked on the altered NIR-FAF response in several retinal dystrophies, but did not describe the functional relationships.[23 25–29]

The interpretation of the mechanisms leading to the alterations of FAF signals is a matter of speculation. FAF, based on the visualisation of lipofuscin and melanin distribution, can provide a metabolic insight into retinal cell dysfunctions in STGD. Intracellular melanin is an important molecule involved in RPE homeostasis.[29] It tends to decrease in the RPE with age, whereas lipofuscin accumulation gradually increases. Thus, the amount of melanin within RPE cells may have an indirect effect on lipofuscin accumulation and/or the photo-oxidation of lipofuscin-related compounds.[30 31]

The pathogenesis of STGD appears to be very complex, involving photoreceptors and RPE cells.[12–19] Overall, final visual acuity, as a direct measurement of visual function, is probably the result of an intricate interaction of impairments at different levels. The preservation of a good melanin distribution within the RPE cells in the fovea may be considered a useful morphological surrogate marker of good photoreceptor-RPE cell activity, especially as several new approaches to treatment will be ready for clinical trials in the near future. We acknowledge that this study has several limitations, especially regarding the limited number of patients and the absence of a follow-up showing the FAF changes over time. Another problem inherent in a study of this kind is the inevitably subjective and qualitative nature of the evaluation of AF. Other obvious limitations of FAF imaging regard the acquisition technique. The quality of the AF images depends on accurate focusing, appropriate illumination, motion artefacts and media transparency, and all these variables may have affected the acquisition and interpretation of the images in our study.

The morpho-functional analysis was carried out considering the BCVA assessment and the microperimetry evaluation. In an advanced stage of STGD, and in many maculopathies, the deterioration of the foveal area also induces a fixation loss. BCVA assessment is the easiest and most direct way of measuring the visual function and is also generally the way of describing eyesight that the patient understands best. However, eccentric or unstable fixation is not the most reliable parameter in evaluating the foveal function. In contrast, microperimetry provides a precise evaluation of threshold sensibility at a specific point. A multimodal analysis is therefore to be preferred in assessing the correlation between the retinal findings and the corresponding visual function. The combined acquisition of FAF and SD-OCT and a comprehensive examination of the visual function may facilitate the monitoring of retinal abnormalities and visual changes in follow-up examinations, which are essential for any future therapeutic strategy.

In essence, our investigation reveals that NIR-FAF patterns correlate with morpho-functional outcomes in eyes affected by STGD. Longitudinal investigations are warranted to ascertain more precisely the actual contribution of NIR-FAF in the clinical characterisation of STGD.

Contributors Contributions of authors in each of these areas: conception and design: MBP; analysis and interpretation: MBP, PI, GT, CLS, IZ, MVC, EB, MPM, EM, FB; writing the article: MBP, PI, GT, CLS, IZ, MVC, EB, MPM, EM, FB; critical revision of the article: MBP, PI, FB; final approval of the article: MBP, PI, GT, CLS, IZ, MVC, EB, MPM, EM, FB; data collection: MBP, PI, GT, CLS, IZ, VCM, EB, MPM, EM, FB; provision of materials, patients, or resources: MBP, PI, GT, CLS, IZ, MVC, EB, MPM, EM, FB; statistical expertise: PI, MBP; literature search: PI, MBP.

Funding The contribution of the Fondazione Bietti in this paper was supported by the Ministry of Health and Fondazione Roma.

Competing interests None.

Patient consent Obtained.

Ethics approval Institutional review boards of the, University Vita-Salute, Scientific Institute San Raffaele, Milano, Italy.

Provenance and peer review Not commissioned; externally peer reviewed.

REFERENCES

1 Rotenstreich Y, Fishman GA, Anderson RJ. Visual acuity loss and clinical observations in a large series of patients with Stargardt's disease. *Ophthalmology* 2003;110:1151–8.
2 Armstrong JD, Meyer D, Xu S, *et al*. Long-term follow-up of Stargardt's disease and fundus flavimaculatus. *Ophthalmology* 1998;105:448–58.
3 Fishman GA, Farber M, Patel BS, *et al*. Visual acuity loss in patients with Stargardt's macular dystrophy. *Ophthalmology* 1987;94:809–14.
4 Allikmets R, Singh N, Sun H, *et al*. A photoreceptor cell-specific ATP-binding transporter gene (ABCR) is mutated in recessive Stargardt macular dystrophy. *Nat Genet* 1997;15:236–46. Erratum in: *Nat Genet* 1997;17:122.
5 Allikmets R, Shroyer NF, Singh N, *et al*. Mutation of the Stargardt disease gene (ABCR) in age-related macular degeneration. *Science* 1997;277:1805–7.
6 Glazer LC, Dryja TP. Understanding the etiology of Stargardt's disease. *Ophthalmol Clin North Am* 2002;15:93–100.
7 Cideciyan AV, Aleman TS, Swider M, *et al*. Mutations in ABCA4 result in accumulation of lipofuscin before slowing of the retinoid cycle: a reappraisal of the human disease sequence. *Hum Mol Genet* 2004;13:525–34.
8 Molday RS. ATP-binding cassette transporter ABCA4: molecular properties and role in vision and macular degeneration. *J Bioenerg Biomembr* 2007;39:507–17.
9 Delori FC, Dorey CK, Staurenghi G, *et al*. In vivo fluorescence of the ocular fundus exhibits retinal pigment hepitelium lipofuscin characteristics. *Invest Ophthalmol Vis Sci* 1995;36:718–29.
10 Delori FC, Staurenghi G, Arend O, *et al*. In vivo measurement of lipofuscin in Stargardt's disease-fundus flavimacualtus. *Invest Ophthalmol Vis Sci* 1995;36:2327–31.
11 Von Ruckmann A, Fitzke FW, Bird AC. In vivo autofluorescence in macular dystrophies. *Arch Ophthalmol* 1997;115:609–15.
12 Lois N, Halfyard AS, Bird AC, *et al*. Fundus autofluorescence in Stargardt macular dystrophy-fundus flavimaculatus. *Am J Ophthalmol* 2004;138:55–63.
13 Gomez NL, Greenstein VC, Carlson JN, *et al*. A comparison of fundus autofluorescence and retinal structure in patients with Stargardt disease. *Invest Ophthalmol Vis Sci* 2009;50:3953–9.
14 Sunness JS, Steiner JN. Retinal function and loss of autofluorescence in Stargardt disease. *Retina* 2008;28:794–800.
15 Cukras CA, Wong WT, Caruso R, *et al*. Centrifugal expansion of fundus autofluorescence patterns in Stargardt disease over time. *Arch Ophthalmol* 2012;130:171–9.
16 Gerth C, Andrassi-Darida M, Bock M, *et al*. Phenotypes of 16 Stargardt macular dystrophy/fundus flavimaculatus patients with known ABCA4 mutations and

evaluation of genotype–phenotype correlation. *Graefes Arch Clin Exp Ophthalmol* 2002;240:628–38.
17 Smith RT, Gomes NL, Barile G, *et al*. Lipofuscin and autofluorescence metrics in progressive STGD. *Invest Ophthalmol Vis Sci* 2009;50:3907–14.
18 MCBain VA, Townend K, Lois N. Progression of retinal pigment epithelial atrophy in Stargardt disease. *Am J Ophthalmol* 2012;154:146–54.
19 Testa F, Rossi S, Sodi A, *et al*. Correlation between photoreceptor layer integrity and visual function in patients with Stargardt disease: implications for gene therapy. *Invest Ophthalmol Vis Sci* 2012;53:4409–15.
20 Keilhauer CN, Delori FC. Near-infrared autofluorescence imaging of the fundus: visualization of ocular melanin. *Invest Ophthalmol Vis Sci* 2006;47:3556–64.
21 Weinberger AWA, Lappas A, Kirchkamp T, *et al*. Fundus near infrared fluorescence correlates with fundus near infrared reflectance. *Invest Ophthalmol Vis Sci* 2006;47:3098–108.
22 Cideciyan AV, Swider M, Aleman TS, *et al*. Reduced-illuminance autofluorescence imaging in ABCA4-associated retinal degenerations. *J Opt Soc Am A Opt Image Sci Vis* 2007;24:1457–67.
23 Kellner S, Kellner U, Weber BH, *et al*. Lipofuscin- and melanin-related fundus autofluorescence in patients with ABCA4-associated retinal dystrophies. *Am J Ophthalmol* 2009;147:895–902, 902.e1.
24 Fishman GA, Stone EM, Grover S, *et al*. Variation of clinical expression in patients with Stargardt dystrophy and sequence variations in the ABCR gene. *Arch Ophthalmol* 1999;117:504–10.
25 Weiter JJ, Delori FC, Wing GL, *et al*. Retinal pigment epithelial lipofuscin and melanin and choroidal melanin in human eyes. *Invest Ophthalmol Vis Sci* 1986;27:145–52.
26 Kennedy CJ, Rakoczy PE, Constable IJ. Lipofuscin of the retinal pigment epithelium: a review. *Eye* 1995;9:763–71.
27 Sundelin SP, Nilsson SE, Brunk UT. Lipofuscin-formation in cultured retinal pigment epithelial cells is related to their melanin content. *Free Radic Biol Med* 2001;30:74–81.
28 Parodi MB, Iacono P, Pedio M, *et al*. Autofluorescence in adult-onset foveomacular vitelliform dystrophy. *Retina* 2008;28:801–7.
29 Duncker T, Tabacaru MR, Lee W, *et al*. Comparison of near-infrared and short-wavelength autofluorescence in retinitis pigmentosa. *Invest Ophthalmol Vis Sci* 2013;54:585–91.
30 Parodi MB, Iacono P, Del Turco C, *et al*. Near-infrared fundus autofluorescence in subclinical best vitelliform macular dystrophy. *Am J Ophthalmol* 2014;158:1247–1252.e2.
31 Parodi MB, Iacono P, Campa C, *et al*. Fundus autofluorescence patterns in best vitelliform macular dystrophy. *Am J Ophthalmol* 2014;158:1086–92.

Morpho-functional correlation of fundus autofluorescence in Stargardt disease

Maurizio Battaglia Parodi, Pierluigi Iacono, Giacinto Triolo, Carlo La Spina, Ilaria Zucchiatti, Maria Vittoria Cicinelli, Enrico Borrelli, Maria Pia Manitto, Elisabetta Martina and Francesco Bandello

Br J Ophthalmol published online April 2, 2015